JOURNAL OF MATERIALS SCIENCE 8 (1973) 1041–1048

The strength and fracture properties of glass-ceramics

P. HING, P. W. McMILLAN
Department of Physics, University of Warwick, Coventry, UK

The effect of an isothermal heat-treatment on the strength and fracture surface energy of a glass-ceramic derived from a lithium silicate glass has been studied. It is found that the strength and effective surface energy for crack initiation increase as the mean free path in the intercrystalline glass decreases. The strengthening and toughening mechanisms are discussed.

1. Introduction

In recent years, considerable effort has been directed to the study of the formation of glass-ceramics [1, 2], yet it is still impossible to generalize on the effect of crystal size on the strength of complex glass-ceramics. In particular, the effect of microstructural parameters on the fracture surface energy is not well documented. One difficulty often encountered in studying the microstructures of glass-ceramics is that the morphologies of the crystalline phases vary significantly with heat-treatment and chemical composition. This arises partly because minor constituents in the glass alter the kinetics of phase separation, nucleation and crystallization, as well as the mineralogical contents of the final glass-ceramics. The crystalline phases may not always correspond to the phases predicted for a particular composition and temperature in the equilibrium phase-diagram. For instance, West and Glasser [3, 4] identified seven polymorphs in the $Li_2O.ZnO.SiO_2$ system that are structurally related to the Li_3PO_4 family. James and McMillan [5, 6] found that the addition of 1 mol % of phosphorus pentoxide in a glass of molecular composition $30\,Li_2O.69SiO_2.1P_2O_5$ alters, markedly, the morphology and number density of the phase-separated droplets. This, in turn, influences the nucleation and crystallization behaviour of the glass [7], resulting in significant improvement in the mechanical strength [8]. Evidence concerning the influence of phosphorus pentoxide on the efficiency of nucleation of lithium disilicate by electron transmission microscopy has been reported by Hing and McMillan [9].

Many of the previous studies were concerned with glasses of simple compositions, but useful glass-ceramics are generally more chemically complex. To simulate more closely such glass-ceramics, a glass of the molecular composition $68SiO_2$, $29Li_2O$, $1ZnO$, $1P_2O_5$, $1K_2O$ was prepared. It was decided to investigate the relationship between the glass-ceramic microstructure and the mechanical strength and fracture surface energy. Of particular relevance to the present work are the papers by Hasselman and Fulrath [10] on the properties of hot-pressed glass-ceramic particle composites and by Frieman and Hench [11] on partially crystallized $70SiO_2.30Li_2O$ glass. Both sets of authors found that the mechanical strength is proportional to the square root of the reciprocal of the mean free path.

2. Experimental techniques

2.1. Glass preparation

The glass was prepared by mixing the appropriate amounts of reagent-grade lithium carbonate lithium phosphate, zinc oxide, potassium nitrate and powdered Brazilian quartz The compositions were melted in 500 g quantities in a platinum −2% rhodium crucible for about 3 h at 1450°C and quenched in water. The resulting "frit" after drying was crushed, mixed and remelted at 1450°C until it was homogeneous and bubble-free The molten glass was cast into slabs 12.5 × 1.5 × 1.5 cm.

2.2. Conversion of glass to glass-ceramic

The slabs after casting were transferred to a furnace at 500°C for a nucleation treatment

of 1 h. This heat-treatment did not alter the transparency of the glass, indicating the absence of significant phase-separation. The slabs were then machined into rectangular beams of 5.8 × 0.7 × 0.5 cm and given an isothermal crystallization anneal at 550°C for periods ranging from 1 to 48 h to convert the glass into glass-ceramic. The machined beams were introduced in the furnace at 550°C and removed from 550°C to ambient after each heat-treatment.

2.3. Determination of mechanical strength and fracture surface energy

Because of the difficulties encountered in machining the crystallized glasses, all the slabs were machined after the nucleation heat-treatment, but before the isothermal treatment at 550°C. The beams were polished down to 1 μm surface finish for mechanical strength measurements. Notches ranging from 0.12 to 0.15 cm were made in the roughly polished beams. The notched and unnotched specimens were fractured at room temperature on a three-point bending jig with a 3.8 cm span between the outer knife edges using an Instron machine, operating at a cross-head speed of 0.02 cm min^{-1}. On average, four specimens were used for each strength and fracture surface energy determination.

The modulus of rupture of a rectangular bar for centre loading is determined from the expression

$$\sigma_F = \frac{3P_F L}{2bd^2} \quad (1)$$

where P_F is the load to fracture, L the distance between the knife edges, b the width and d the thickness of the bar. The Young's modulus in bending is determined from the force/deflection curve using the expression

$$E_b = \frac{PL^3}{4bd^3y} \quad (2)$$

where y is the deflection corresponding to load P. The effective surface energy for crack initiation, γ_I is determined from

$$\gamma_I = \frac{9P_F^2L^2Y^2c}{8E\,b^2d^4} \quad (3)$$

Equation 3 is obtained by combining Equation 1 and Brown and Scrawley's [12] modified Griffith equation given by

$$\sigma_F = \frac{1}{Y}\left[\frac{E(2\gamma_I)}{c}\right]^{\frac{1}{2}} . \quad (4)$$

P_F here refers to the fracture load of the notched bar; Y is a numerical factor depending on the geometry of the specimen which can be easily calculated and c is the crack length. This method of evaluating the fracture surface energy for crack initiation for brittle material has been used by previous workers [13-16]. The validity of using Equation 3 for determining γ_I has been discussed and justified [13, 14]. This point is further discussed in Section 4.

2.4. Stereological parameters

The morphology of the crystalline phase was examined by optical, scanning and electron microscopy. The crystalline phase was revealed by etching the surface, after polishing down to 1 μm finish, with a solution of 3HF.2HCl. $95H_2O$. Scanning electron microscopy of the etched polished surface and unetched fracture surface was carried out after lightly coating with aluminium to prevent charging. The mean free path, λ, was determined using the relation [17].

$$\lambda = \bar{L}\left(\frac{1 - V_f}{V_f}\right) \quad (5)$$

where V_f is the volume fraction of the crystalline phase, $\bar{L}$ is the average particle size. The crystalline phase present was identified by X-ray powder diffraction of part of the fractured beams. Confirmation of the crystalline phase was obtained by selected-area diffraction of thin foils prepared by a technique reported earlier [9].

3. Results

3.1. Microstructures

The major crystalline phase developed at 550°C has been identified as lithium disilicate by X-rays and electron diffraction. The morphology of the crystals varies distinctly with different periods of crystallization as shown in Fig. 1 a, b and c) and Fig. 2a and b. The relevant stereological parameters are shown in Table I. It is interesting to note that the volume fraction initially increases with duration of heat-treatment but remains fairly constant between 24 and 48 h heat-treatment. The maximum number density of the crystals ($\sim 1.0 \times 10^{16}\ m^{-3}$) with an average grain size of 4.0 μm occurs for the 24-h-crystallized glass. The fracture

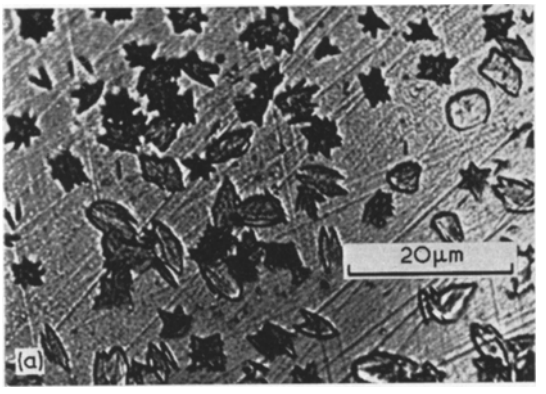

surfaces of crystallized glasses are considerably rougher than the uncrystallized glass as shown in Fig. 3a, b and c and fracture occurs mainly in a transgranular fashion with occasional pull-out of the grains. It is observed that multiple sharp flaws exist at the base of the machined notches for uncrystallized glasses (Fig. 4), whereas the flaws are hardly detected in the case of crystallized glasses.

3.2. Mechanical properties

The mechanical strength of the material increased progressively with duration of heat-

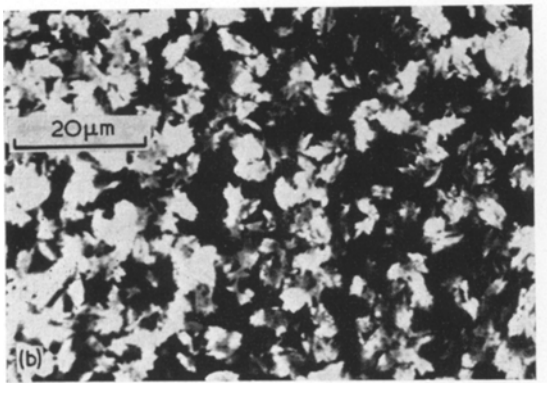

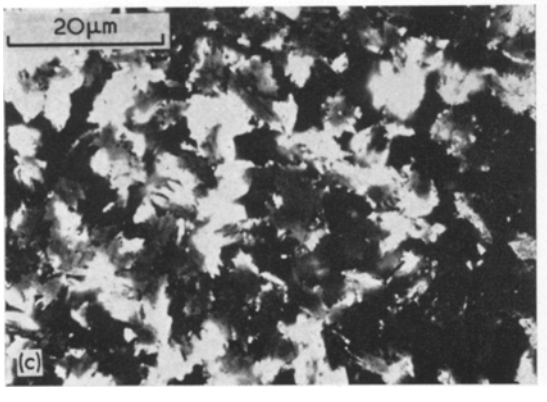

Figure 1 Morphology of lithium disilicate crystals. All specimens were given a nucleation treatment of 500°C for 1 h followed by a crystallization treatment of (a) 550°C for 1 h, (b) 550°C for 24 h and (c) 550°C for 31.5 h.

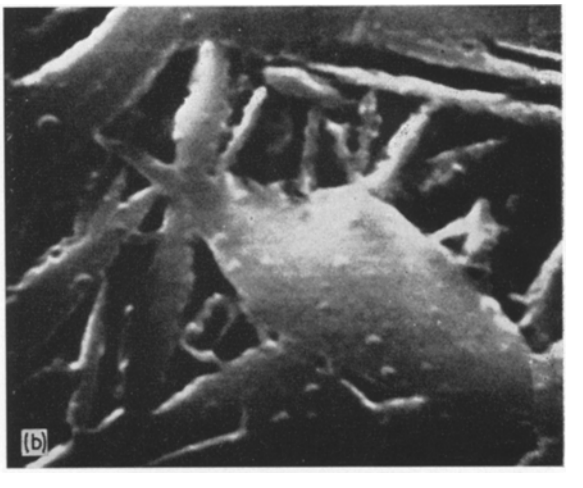

Figure 2 Scanning micrographs showing the morphology of lithium disilicate crystals (a) 550°C for 6 h, × 1100; (b) enlarged view of (a), × 10700. The glass was given a nucleation treatment of 500°C for 1 h.

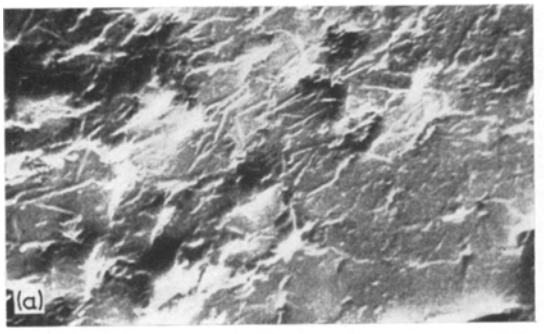

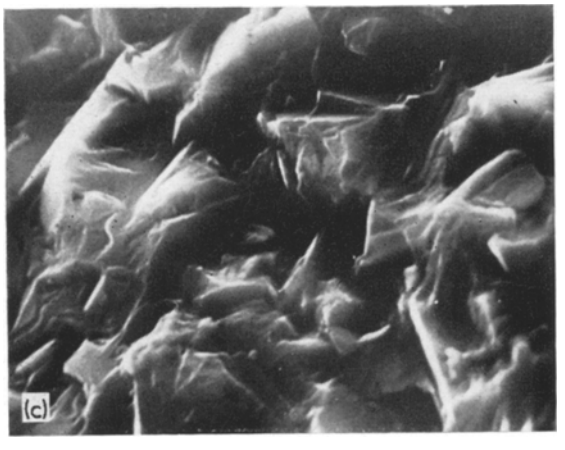

Figure 3 Scanning micrographs of the fracture surfaces or (a) uncrystallized glass, × 2700; (b) crystallized glass after 500°C for 1 h and 550°C for 6 h × 4000; (c) after 500°C for 1 h and 550°C for 24 h ×4400.

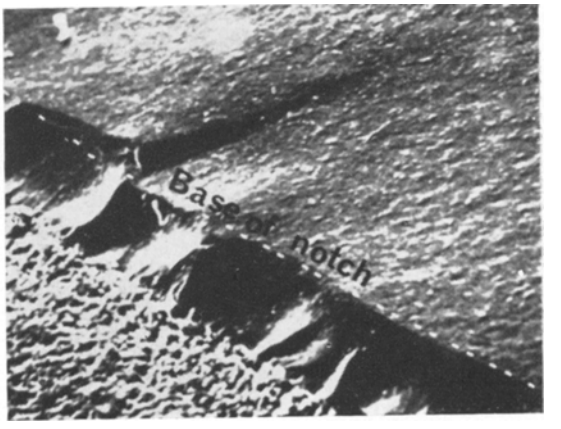

Figure 4 Scanning micrograph showing flaws at the base of a machined notch in an uncrystallized glass, × 120.

treatment at 550°C up to 24 h, when it was higher than that of the uncrystallized glass by a factor of two (Fig. 5). Further heat-treatment caused a reduction of strength. Similarly the fracture surface energy increased to a maximum of about six times that of the uncrystallized glass after 24 h heat-treatment. It was noted that the glass-ceramics behaved elastically up to fracture using both notched and unnotched specimens.

Determination of the stereological parameters enabled the relationships between mechanical strength and the square root of the reciprocal of the mean free path shown in Fig. 6 to be established. A relationship between the fracture surface energy and the reciprocal of the mean free path is suggested by the plot shown in Fig. 7.

It was also noted that the Young's modulus determined in bending increased to a maximum value of about 6.3×10^4 MN m^{-2} after 24 h heat-treatment. The micro-indentation hardness (Vickers) for a standard load of 200 g and 15 sec loading time increased from 2.2×10^3 to 3.1×10^3 MN m^{-2} after heat-treatment for 1 h at 550°C but thereafter no further change occurred in this parameter.

4. Discussion

4.1. Mechanical strength

The high mechanical strength of glass-ceramics is often ascribed to their fine-grained microstructures and it has been assumed that the finer the grain size, the higher the mechanical

strength. In fact, it has been suggested that the mechanical strength is related to the mean grain diameter, d, by the relationship [18]

$$\sigma = K_1 d^{-\frac{1}{2}} \quad (6)$$

where K_1 is a constant. The implication of Equation 6 is that the crack length in the Griffith equation

$$\sigma = \left[\frac{2E\gamma}{\pi c}\right]^{\frac{1}{2}} \quad (7)$$

has the same dimension as the grain diameter. This might suggest that the critical flaw is within the crystalline phase. However, it can be seen from Table I that d does not vary much with annealing time and does not correlate with σ_F. The results from the present study indicate that the strength is more intimately related to the mean free path, λ, in the inter-crystalline glass, i.e.,

$$\sigma = K_2 \lambda^{-\frac{1}{2}} \quad (8)$$

where K_2 is a constant and λ is given by Equation 5. Equation 8 implies that microcracks exist only in the glass, being terminated by the crystal boundaries and having dimensions of the mean free path. Hench *et al* [11] have reported a similar dependence of strength on the mean free path in a partially crystallized glass of molecular composition $70SiO_2.30Li_2O$. The result as expressed in Equation 8 is also consistent with the work of Fulrath *et al* [10] on hot-pressed glass-ceramic particle composites.

One interesting feature observed is that significant strengthening occurs for a relatively coarse-grained glass-ceramic. For instance, an optimum strength of 343 ± 12 MN m^{-2} was noted in crystallized glasses containing crystals having an average size of 4 μm after a 24-h crystallization heat-treatment. The flat region of the strength versus $\lambda^{-\frac{1}{2}}$ curve in Fig. 6 indicates that for low volume fraction of second phase, the strength is probably very weakly dependent on the mean free path. The discontinuity in the strength curve can be used to estimate the mean critical flaw size in the glass. This turns out to be about 10 μm. The rising part of the strength versus $\lambda^{-\frac{1}{2}}$ curve shows that for significant strengthening, the values of λ must be quite small. If this dependence is correct, then for the strongest specimen the flaw size, c, estimated from the modified Griffith equation,

$$\sigma_F = \frac{1}{Y}\left[\frac{E(2\gamma_I)}{c}\right]^{\frac{1}{2}}$$

for $\sigma_F \sim 343$ MN m^{-2}, E $\sim 6.3 \times 10^4$MN m^{-2}, $\gamma_I \sim 97$ J m^{-2} should be close to the corresponding mean free path. The value of c, about 3 μm, obtained in this way is sufficiently close to λ(2.2 μm) to support the argument that the strength of the glass-ceramic is controlled mainly by the critical flaw size in the residual glass phase. The severity and size of these flaws are then controlled by the bulk microstructural parameters.

Alternative explanations for the strengthening resulting from heat-treatment up to 24 h could be proposed. For instance it could be argued that since the Young's moduli of the crystallized glasses are higher than that of the parent glass theories based on the critical strain concept

TABLE I Mechanical properties of glass-ceramics material 68 SiO_2.29 LiO.1 ZnO.1 P_2O_5.1 K_2O

Heat-treatments. All specimens given a nucleation heat-treatment at 500°C for 1 h, followed by 550°C for different times (h)	Mechanical strength. three-point bending, σ_F (MN m^{-2})	Effective surface energy for crack initiation, γ_I (J m^{-2})	Young's modulus in bending E_b (10^4 MN m^{-2})	Mean free path, λ (μm)	Average crystal size, d (μm)	Number of particles per m^3 ($\times 10^{15}$)	Volume fraction of crystalline phase
0	176 ± 15.0	16.6 ± 9.8	3.35	—	—	—	—
1	176 ± 10.8	48.2 ± 4.0	3.76	8.3	4.6	4.6	0.35
6	266 ± 15.7	76.0 ± 8.6	4.40	5.1	5.1	5.1	0.52
10	258 ± 11.3	67.6 ± 4.4	4.76	3.5	4.2	9.3	0.60
16	281 ± 12.7	81.0 ± 15.0	5.34	3.6	3.5	10.0	0.60
24	343 ± 12.0	97.0 ± 16.5	6.34	2.2	4.0	10.0	0.67
31.5	286 ± 17.0	83.9 ± 13.2	5.00	3.0	6.5	3.6	0.65
48	239 ± 20.6	66.2 ± 15.0	5.27	4.2	5.3	3.0	0.60

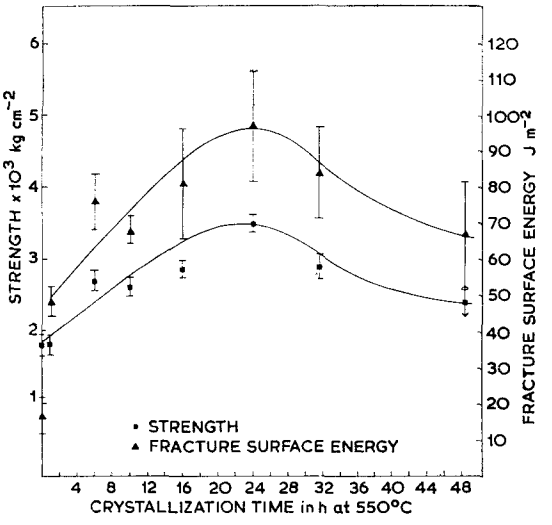

Figure 5 Effect of crystallization time at 550°C on the strength and fracture surface energy. All the specimens were given a nucleation heat-treatment of 500°C for 1 h.

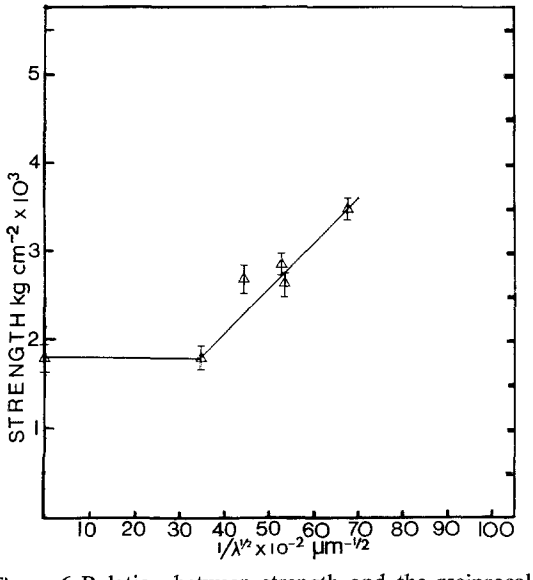

Figure 6 Relation between strength and the reciprocal of the square root of the mean free path.

should predict a higher strength for the glass-ceramics. This explanation is, however, insufficient since the glass-ceramics are stronger than the glass by a much larger factor than the ratios of the elastic moduli. Significant strengthening of the glass-ceramics owing to the generation of compressive stresses in the material as a result of differential thermal contraction of the crystal phase and the residual glass phase is rather unlikely in the present case since the

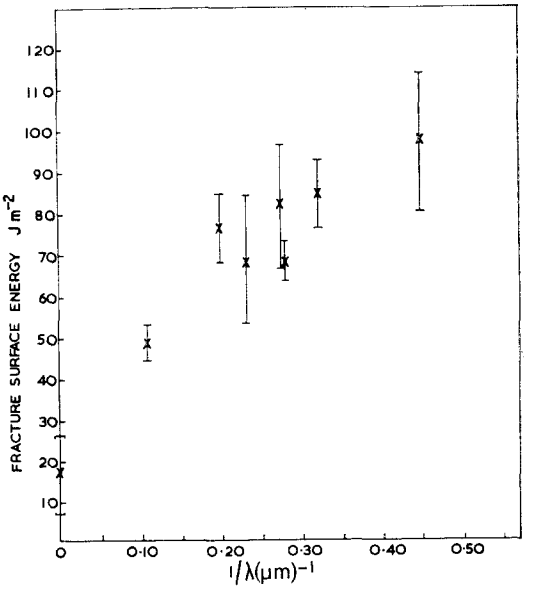

Figure 7 Fracture surface energy versus reciprocal of the mean free path.

difference between the coefficients of expansion of the two phases is thought to be small [8].

The decrease in the strength for glasses crystallized between 24 and 48 h could be attributed to coarsening of the lithium disilicate crystals while the volume fraction remain fairly constant. Hench *et al* [11] have, however, attributed the decrease in strength with prolonged crystallization heat-treatment of the $70SiO_2.30Li_2O$ glass to the development of localized cracks at the crystal-glass interface as a result of volumetric changes during crystallization. Cracking of this kind has not been observed in the present glass-ceramic. It is possible that the addition of a small amount of potassium oxide plays an important role in relieving any localized stress, thereby reducing or eliminating the possibility of localized cracking.

4.2. Effective surface energies for crack initiation

4.2.1. Subsidiary cracking

The slope of the strength versus $\lambda^{-\frac{1}{2}}$ curve in Fig. 6 should give an estimate of the surface energy term γ in the Griffith equation which describes the macroscopic fracture strength of brittle materials. Using a value of $E \sim 6.3 \times 10^4$MN m^{-2}, then $\gamma \sim m^2/E \sim 4$ J m^{-2}, where m is the slope of the strength versus $\lambda^{-\frac{1}{2}}$ curve.

The value of γ for the glass phase is significantly lower than γ_I, the effective surface energy for crack initiation for the uncrystallized glass. The value of γ_I, of 16 J m^{-2}, found experimentally for the glass indicates that additional energy absorption occurs during fracture and this could be associated with the configuration of the flaws at the base of the notch. It is thought that this enhancement in the values of γ_I is due to subsidiary cracking at the base of the machined notches. The presence of multiple crack initiation sites frequently observed in the glass supports this suggestion. High values of γ_I for soda lime glasses [12, 20, 21] may be attributed to this mechanism of energy absorption.

4.2.2. Segmentation of the crack front by crystalline phase

The effective surface energies for the crystallized glasses displayed in Fig. 3 can be represented by

$$\gamma_{GC} = \gamma_G + \frac{k}{f(\lambda)} \quad (9)$$

where γ_{GC} and γ_G are the effective surface energies for the glass-ceramics and the glass, k is a constant. Equation 9 implies that some interactions of the crack with the particles occur. Lange [19] has proposed a theory for the toughening of brittle-matrix composites which involves the segmentation of the crack front at spherical particles and found that the fracture surface energy is linearly related to the reciprocal of the mean free path, given by

$$\gamma_C = \gamma_S \left(1 + \tfrac{2}{3} \frac{C}{\lambda}\right) \quad (10)$$

where C is the flaw size, γ_C and γ_S are the effective surface energies for the composite and the single phase materials, respectively. The results plotted in Fig. 7, despite the scatter, suggest a departure from linearity which could be due to variation in the morphology and the elastic moduli. This mechanism of energy absorption is, moreover, inadequate to account the sixfold increase in the effective surface energies.

4.2.3. Fracture roughness and misorientation of the crystals

Since optical examination of the base of the machined notches in crystallized glasses show the absence of sharp flaws, it is thought likely that the severity and size of these flaws are restricted by the crystalline phases in the glassy matrix. A reduction in the severity of the flaws can arise when the crystalline phases are stronger than the glassy phase or the tips of the flaws are blunted at the glass/crystal boundaries. However, little is known about the internal stress in the glassy regions surrounding the crystalline phases or the glass/crystal interface. The strength of the interface would certainly be affected by differences in the coefficients of expansion, elastic moduli or segregation of impurities at the interface during crystal growth. A slightly weakened interface, nevertheless, would confer some beneficial effect on the fracture toughness of the final glass-ceramics. There is some microstructural evidence to indicate that occasional deflection of the crack along the glass/crystal interface (Fig. 3b) does occur. Stewart *et al* [23] and Utsumi [24] have also observed deflection of the cracks by the lithium disilicate crystals. However, since most of the crystalline phases in the present glass-ceramic undergo transgranular fracture, the morphology of the crystalline phases must play a significant role in the fracture of the glass-ceramics.

Another mechanism which could cause an increase in the effective surface energies arises from the random orientation of the lithium disilicate crystals. Lithium disilicate has an orthorhombic crystal structure with a well-defined cleavage along the (010) plane. For crystals oriented such that crack propagation occurs along the (010) cleavage plane, the increase in the effective surface energies resulting from the formation of the cleavage steps would not be very significant. In the case of crystals oriented such that their cleavage plane is normal to the direction of crack propagation or the applied stress is parallel to the cleavage plane, more resistance would be encountered in propagating a crack across the crystal. For a simple morphology and a very weakly bonded small crystal, the crack would most probably be deflected across the interface with insignificant energy absorption. Because of the irregular morphology and random orientation of the lithium disilicate, the latter can be considered to be rigidly trapped in the continuous glassy matrix. Rupture of the interlocking crystals is expected as a result of release of elastic energy by the advancing crack. This would explain the essentially transgranular fracture of the lithium disilicate. The increase in the fracture roughness probably results from the cleavage along the (010) plane at an angle to the direction of the

crack propagation and subsequent deflection of the crack across the glass/crystal interface. An increase in the stress is therefore needed to rupture these randomly oriented crystals, thus increasing the effective surface energies by a factor equal to the average of $1/\cos^4 \Phi$, where Φ is the angle between the normal to the cleavage plane and the applied tensile stress. It should be noted, however, that the possibility of rupturing some lithium disilicate crystals along other high-index planes rather than the (0 1 0) plane cannot be completely excluded.

5. Summary and conclusion

The mechanical strengths measured for a series of internally crystallized glasses (glass-ceramics) were found to increase as the inverse of the square root of the mean free path in the glass. This suggests that microcracks exist in the glass phase having a mean length equal to the mean free path, indicating that the crystal boundaries serve to limit the lengths of the microcracks. Although the results show that initiation of fracture is in the glass phase, the effective surface energy for crack initiation is considerably higher for the glass-ceramics than the original glass. The enhancement in the energy absorption in the glass-ceramics is attributed to a combination of several factors, namely, subsidiary cracking, segmentation of the crack by the crystalline phase, misorientation of the crystals with respect to the fracture path and increase of the fracture surface area. Further investigation is required in order to distinguish the relative importance of these various factors.

Acknowledgements

The authors wish to thank the Science Research Council for financial support and also thank Professor A. J. Forty for his interest and encouragement. One of us (P. W. McMillan) also thanks the Royal Society for the award of a Warren Research Fellowship that enabled his participation in the research.

References

1. S. D. STOOKEY, Paper Presented to Symposium on Nucleation and Crystallization in Glasses and Melts, Amer. Soc (1962).
2. P. W. MCMILLAN, "Glass-Ceramics" (Academic Press, New York, 1964).
3. A. R. WEST and F. P. GLASSER, *J. Mater. Sci.* **5** (1970) 557.
4. *Idem, ibid* **5** (1970) 676.
5. P. F. JAMES and P. W. MCMILLAN, *Phys. Chem. Glasses* **11** (1970) 53.
6. *Idem, ibid* **11** (1970) 64.
7. H. HARPER, P. F. JAMES, and P. W. MCMILLAN, *Discuss. Faraday Soc.* **50** (1970) 206.
8. P. W. MCMILLAN, B. P. HODGSON, and R. E. BOOTH, *J. Mater. Sci.* **4** (1969) 1029.
9. P. HING and P. W. MCMILLAN, *ibid* **8** (1973) 340.
10. D. P. H. HASSELMAN and R. M. FULRATH, "Ceramic Microstructures", in Proceedings of The Third International Materials Symposium, University of California, Berkeley (Wiley, New York, 1966).
11. S. W. FRIEMAN and L. L. HENCH, *J. Amer. Ceram. Soc.* **55** (1972) 86.
12. W. F. BROWN and J. E. SCRAWLEY, ASTM, Special Technical Publication No. 410 (1967).
13. R. W. DAVIDGE and G. TAPPIN, *J. Mater. Sci.* **3** (1968) 1962.
14. R. W. DAVIDGE and A. G. EVANS, *Phil. Mag.* **20** (1960) 373.
15. *Idem, J. Mater. Sci.* **5** (1970) 210.
16. P. HING and G. W. GROVES, *ibid* **7** (1972) 427.
17. R. L. FULLMAN, *Trans. AIME* **197** (1953) 81.
18. Y. UTSAMI and S. SAKKA, *J. Amer. Ceram. Soc.* **53** (1970) 286.
19. F. F. LANGE, *Phil. Mag.* **22** (1970) 983.
20. J. NAKAYAMA, *J. Amer. Ceram. Soc.* **48** (1965) 583.
21. E. B. SHAND, *ibid* **44** (1961) 167.
22. F. LIEBAU, *Acta. Cryst.* **14** (1961) 395. *ibid* **14** (1961) 389.
23. I. M. STEWART, I. BROUGH, and L. GREEN, *J. Mater. Sci.* **3** (1967) 63.
24. Y. UTSUMI, *Yogyo-Kyokai-Shi* **1** (1971) 79.

Received 28 November and accepted 22 December 1972.